Nuclear Inst. and Methods in Physics Research B 478 (2020) 125–130

Contents lists available at ScienceDirect

Nuclear Inst. and Methods in Physics Research B

journal homepage: www.elsevier.com/locate/nimb

Oscillating behavior of proton scattering amplitude on an electron-stimulated-desorbed surface of KBr by keV electrons

Yuuko Fukazawa*, Kenya Tasaki, Yasufumi Susuki

Division of Science Education, Osaka-Kyoiku University, Kashiwara, Osaka 582-8582, Japan

ARTICLE INFO

Keywords:
Surface scattering of ions
Alkali-Halide
Electron stimulated desorption
Layer-by-layer desorption
X center
F center

ABSTRACT

Specular yields of 15 keV protons scattered from a KBr(0 0 1) electron-stimulated desorbed surface for 1.5–5 keV electron irradiation have been measured, whose periodic oscillations are resulting from the layer-by-layer removal by surface erosion. In each oscillation, the first half-period is found to elongate compared with subsequent half-periods. This elongation indicates that extra electron fluence is needed for the initiation of the surface erosion. The elongation depends on the irradiation electron energy and decreases with the elevating temperature of the sample. From the extra electron fluence irradiated during the elongation, the amount of F centers accumulated in the thin surface layers rise to 30% of the number of alkalis on the topmost layer. This high number of F centers indicates that, before the initiation, the growth of aggregated F centers takes place in numerous heaped F centers under the flat surface, as though the X centers are sinks of F center-diffusion.

1. Introduction

Ion beam analysis of surface nanostructures has been applied to clarify a number of characteristics (e. g., atomic arrangements, relaxation, rumpling, lattice vibration) [1]. Using proton beams, we have investigated the morphology resulting from the electron-stimulated desorption (ESD) of an alkali-halide cleaved surface (ESD surface) [2,3].

It is known that the alkali-halides ESD surface irradiated by keV electrons contains many rectangular pits that is formed via the so-called “layer-by-layer” desorption [4]. In the surfaces, a number of F and H center pairs are created as Frenkel defects by external electrons, where the F center is formed by an electron trapped in a halogen vacancy and H center is formed by an interstitial halogen atom. The defects, H and F* (2p excited F center, which is movable) centers, diffuse to the topmost surface, and F centers aggregate on the surface. The aggregated F center is hypothetical object named X center, initiates the formation of a small pit (initial pit). After the initial pit density on the surface is saturated, the removal of the first layer proceeds by expanding the area of each pit. This is because only the alkali atoms on low coordinate states can be neutralized by F centers and the number of the low coordinated atoms is increased by the pit formation. At the same time, when the neutralized alkali atom is ejected, the adjacent halogen atom is replaced by the F centers [5].

For a novel application of this mechanism for alkali halides, F and X center dynamics was discussed in the context of highly charged ions (HCIs) irradiation [6]. KBr crystal was used to count HCIs via the observation of pits on the surface irradiated by HCIs [6,7]. The ion approaching the surface acts as a point source of potential sputtering and a source for energetic electrons via the Auger process. The pits are formed on the KBr surface with high efficiency by the ion. Thus the surfaces were used as a detector for counting HCIs. A detail of X center dynamics was begun to discuss, e. g., possible shapes of the X centers created in the KCl surface induced by HCIs [8].

Although the previously mentioned ESD scenario is generally accepted, the model for the ESD scenario does not completely describe all aspects of ESD of alkali halides [9]. In spite of the application concerning with the pits, the mechanism of the initial pit formation is a representative one that remains unclear and requires further investigation. For example, the pit formation requires the aggregated F (X) centers at the start of the periodic removal of the surface layers. Since the X centers are hypothetical objects, it is not clear why F centers aggregate to form X centers or why and when they initiate the formation of pits on the flat surface. For the application of the pits to study interactions of HCIs with surface, the ion above the surface acts as a point source electrons [6–8]. The formation of the X centers by HCIs relates deeply with the results of ESD by ordinary electron impacts. In this work, we measured the specular oscillation of protons scattered on a KBr(0 0 1) ESD surface following the periodical removal of layers to enhance our understanding of the mechanism of ESD. We used a 15 keV

* Corresponding author.
E-mail address: yukofu@cc.osaka-kyoiku.ac.jp (Y. Fukazawa).

https://doi.org/10.1016/j.nimb.2020.05.021
Received 27 February 2020; Received in revised form 4 May 2020; Accepted 22 May 2020

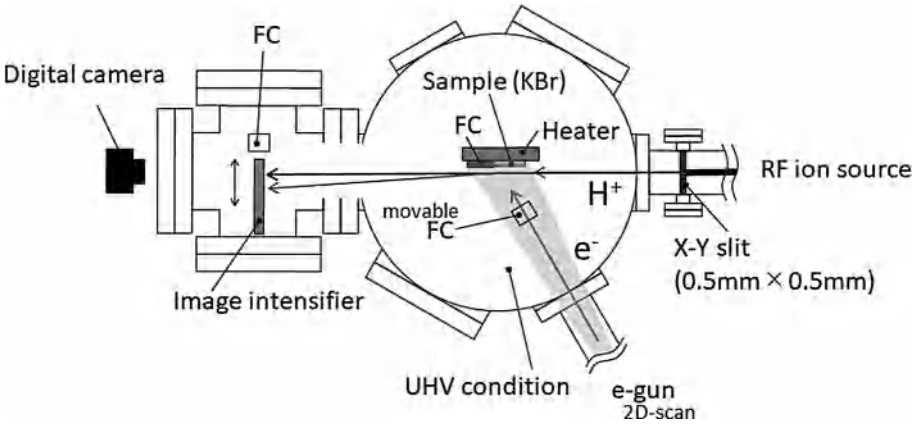

Fig. 1. A schematic depiction of the experimental setup.

proton beam for ion scattering and the energy of the electrons for irradiation was 1.5–5 keV.

2. Experimental procedure

The experimental setup for the proton beam was described in our previous work [10,11]. The proton beam from a radio frequency ion source was transported to an ultra-high-vacuum (UHV) chamber through two sets of X–Y slits. The base pressure of the UHV chamber was 1×10^{-7} Pa.

Fig. 1 shows the schematic expression of the sample, electron irradiation and proton scattering experiments. The KBr sample ($22 \times 17 \times 4$ mm^3) was cleaved along the (0 0 1) surface in air and was mounted on a sample holder with a four-axis goniometer. To clean the surface, the sample was heated to 425 K and was maintained at this temperature for 24 h (simultaneously baking the UHV chamber). Further, the sample was heated to 580 K and maintained at this temperature for 1 hr. Measurements were performed on the several cleavage surfaces of the KBr sample. The identical surfaces were cleaned between the subsequent experiments using the same procedure (to be heated to 580 K for annealing at 1 h). Measurements using the identical surface were made 5–15 times.

The sample temperatures were measured at the heater, near where the sample was positioned, using a thermocouple set. Although our data with the heater temperature are shown for the purposes of comparison with other previously reported results [4,5], the surface temperature of the sample was lower than the heater temperature because of the contact heat-resistance between the sample and the heater. The difference was estimated to be from 5 K (at 360 K) to 20 K (at 460 K) [12]. This estimation did not depend so much on the experimental setup such as the vacuum chamber or the sample thickness, but decreased slightly with the increasing force involved in clip the sample onto the heater.

The sample surface was irradiated by 1.5–5 keV electrons from a gun connected to a port of the UHV chamber with an incidence angle of 60° measured from the (0 0 1) surface. At the entrance of the port of the chamber, the electron beam was collimated by a 1.5×10 mm^2 slit and scanned two dimensionally by a modulated line scan method. The electron beam after the scanning was spread over an area of 35×30 mm^2 in front of the sample, and it covered the whole surface. The current density was in the range of 40 ± 15 nA cm^{-2}, which was adjusted using two sets of Faraday cups with electron suppressors: one was connected to a ceramic fixed behind an aperture of a movable fluorescent screen, which also operated as an electron suppressor, and another set was fixed 4 mm above the sample on the sample holder.

Interrupting the electron irradiation, the 15 keV proton beam collimated to 0.5×0.5 mm^2 by two sets of X–Y slits impinged on the surface with angles θ_i of $0.65° \pm 0.15°$. The azimuthal angle of the incident beam was set off by 6° from the [1 0 0] crystallographic axis on the surface. The incident beam currents after the collimation were no more than 10 pA. The scattered beam was observed as a scattering pattern. That is, the patterns on the fluorescent screen placed behind a micro-channel plate (MCP) were measured by capturing images with a commercial digital camera (EOS 60D; Canon). The intensity distributions of the scattered patterns were obtained from the B values of the RGB color values of the images. Each image was obtained via a summation of 4 pictures. Each picture was exposed for 30 s. Between them, 35 s intervals were needed for computer processing to make image data from the taken picture. Since time for irradiation of electrons was needed, a total of 8 min, which includes the acquisition and the processing time, was required for each set of irradiation fluence. Fig. 2 shows an example of the images measured by the digital camera. In the image depicted, the incident beam was synthesized with the scattering beam. As the current density of the incident beam was too large to be measured by the MCP, the bias voltage for the incident beam to the MCP was suppressed.

The specular intensities, captured in window A in Fig. 2, were normalized by the total scattering intensities in window B, and were plotted as normalized specular yields with increasing electron fluence. Fig. 3 shows examples of the normalized specular yields. For comparison, the specular yield at the non-irradiated surface is also shown in Fig. 3(a), where the yield was found to be constant for the number of measurements (i.e., the irradiation of protons). This is evidence that the protons did not give any detectable damage on the surface. The yields for the electron irradiated surface showed damping oscillations. They are shown in Fig. 3(b)–(d) with fitting curves obtained using statistical

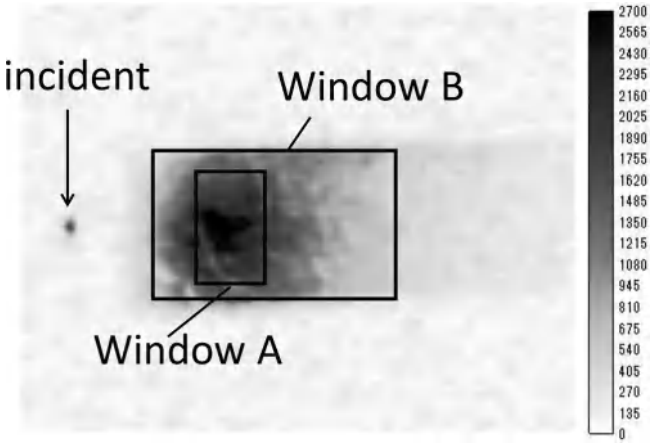

Fig. 2. An example of the scattering patterns. The B value of the RGB color in window A is specular intensity and the B value in window B refers to the total intensity. The width of window A was 16×8 mrad^2.

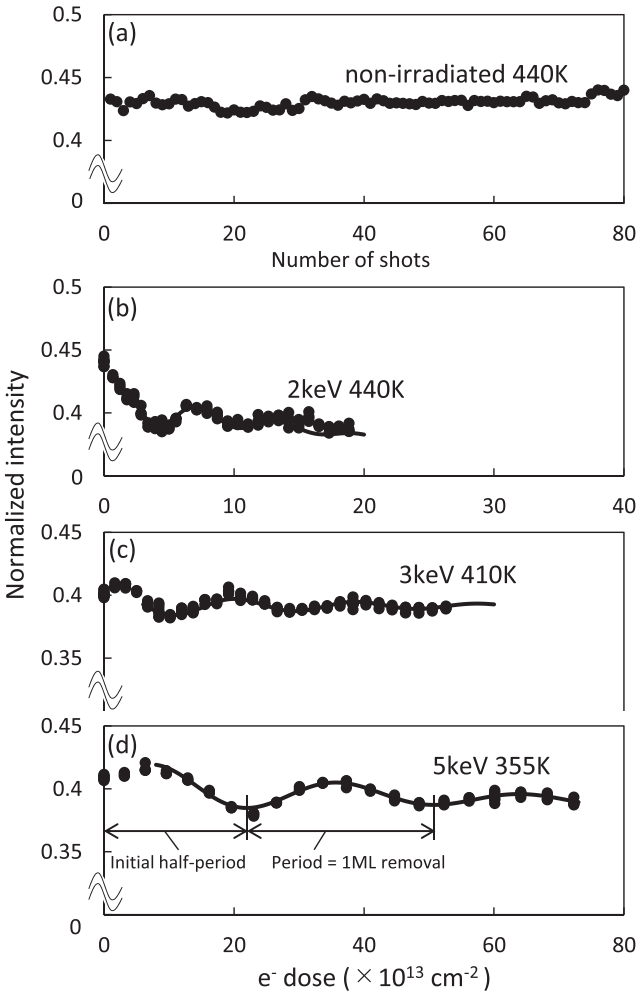

Fig. 3. Examples of the specular yield oscillations for various temperatures. (a) The specular yield at a non-irradiated surface. The specular yield oscillations for (b) 2, (c) 3, and (d) 5 keV electrons. The curves for the oscillation were fitting functions (damping oscillation functions) processed by a statistical program tool. The plots in the initial region were rejected for the fitting, where the curves drawn were truncated.

software referred to as R (R-3.3.2). In all curves, the initial half-periods were elongated compared with those following later.

3. Results

The oscillatory behaviors of the specular intensities were measured according to a variety of energies of irradiating electrons, E_e, and sample temperatures, T. The initial elongations made various shapes of curves (i.e., non-symmetric peaked shapes, flat shapes, or decline shapes) in the first half-periods. In contrast, the steady-state period was not changed by repetition of the cycles but was constant for each condition of E_e and T. The steady-state periods were measured as functions of E_e and are shown in Fig. 4 for three temperatures, T.

Previous results presented by other groups for 1 keV electron irradiation with 45°angle of incidence, where the authors observed oscillatory behaviors of the desorption yields of K and Br atoms, did not show explicit elongated half periods [4,5]. Even if, after the cleaning process in the present study, the surface contained residual pits, adatoms, or molecules, the imperfections were the same for each condition because the annealing processes were the same. In contrast, the elongations did not have the same size but exhibited dependence on E_e and T shown in the next figures (Figs. 5 and 6). The dependence could not be explained by the imperfections of residual pits, adatoms or molecules. In addition, the possibility for residual pits was lower, because the elongations were observed in the first measurements after the sample exchange.

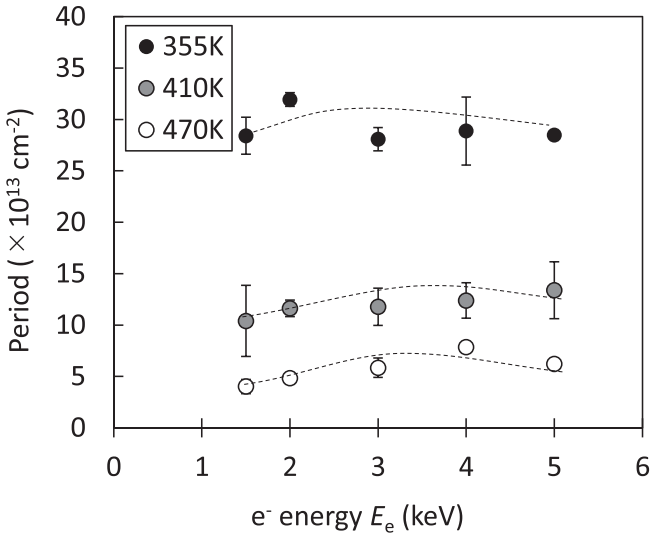

Fig. 4. External electron energy dependence for the periods of steady-state damping oscillations other than the first half. The errors shown were statistical errors obtained by the fitting curves. The standard deviations arising from averaging data measured with the same conditions were also accounted for. The current densities of electrons were 40 ± 15nA cm^{-2}. The three dotted curves are visual guides.

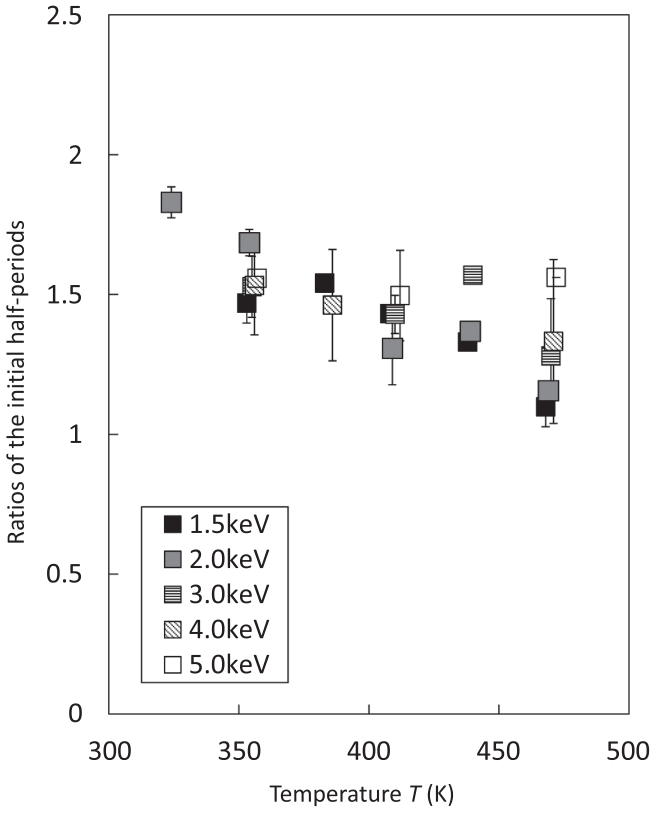

Fig. 5. Dependence of the initial half-periods relative to the other half-periods on the sample temperature, T. The errors shown were statistical errors obtained by the fitting curves. The standard deviations arising from averaging data measured with the same conditions were also accounted for. The five symbols each correspond to E_e. The current densities of electrons were 40 ± 15nA cm^{-2}.

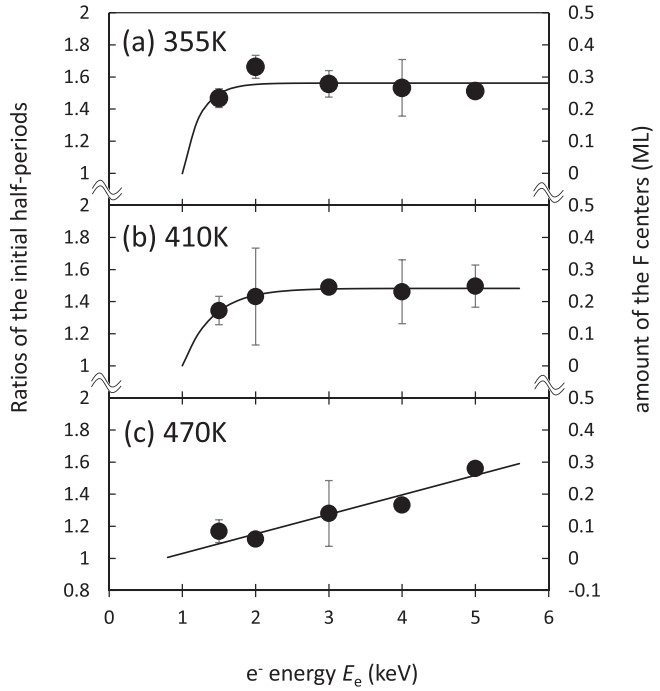

Fig. 6. Dependence of the initial half-periods relative to the other half-periods on the incident electron energy, E_e. The values for T = (a) 355, (b) 410 and (c) 470 K. The errors shown were statistical errors obtained by the fitting curves. The standard deviations arising from averaging data measured with the same conditions were also accounted for. The line in (c) shows a fitting linear function, and the lines in (a) and (b) show the fitting exponential asymptote functions calculated by the data shown along with unity at E_e = 1 keV. The right ordinates of the figures show the number of F centers that accumulated in the thin surface layers before the start of the steady-state damping oscillation in the unit of ML (1 ML is 5.0×10^{14} atoms cm^{-2}). The current densities of electrons were 40 ± 15 nA cm^{-2}.

Fig. 5 shows the temperature dependence of the elongations of the initial half-periods to the other half-periods following (ratios of the initials relative to the others). It can be seen that the elongation decreased with the elevating temperature. Fig. 6 shows the energy dependence of the elongation from those shown in Fig. 5, where the plots are averaged between several measurements in the same conditions. The elongations shown in Fig. 6(a) and (b) were observed to be a few tens of percent and looked like almost constant ratios. Yet, the results in Fig. 6(c) showed an increase of elongation with E_e. The exponential asymptote functions fitted by the data together with unity at E_e = 1 keV are shown in Fig. 6(a) and (b), where we approximated that the previously measured elongation by other groups at 1 keV was negligibly small [4,5,13]. The agreements of the fitting curves with measured plots were good. Thus the previous results appear successively on the present E_e dependence. Therefore the overall results show that, for the low temperature results of Fig. 6(a), the elongation increased with increasing E_e and reached a maximum 1.5–2 keV. In addition, the electron energy, where the elongation reached the maximum, increased with the elevating temperature, T.

Note that, in the previous results for E_e = 1 keV, the density of stored F centers in the surface layers was estimated to be a few percent. The authors did not observed explicit elongation of the first half-period but derived it from the difference between the emission yields of K and Br atoms [4,5,13]. They successfully revealed the amounts of the stored F centers, 0.5–2 $\times 10^{13}$ cm^{-2}, in a few periodic cycles for E_e = 1 keV [5].

4. Discussion

The periods shown in Fig. 4 are proportional to the reciprocals of the yields of atoms desorbed per external electron. The periods reduced with elevating temperature, T. This indicates that the yields of desorption increased with T. Energy dependence of the desorption yields of thermal halogen components was reported previously and had broad minimum at E_e = 2–3 keV [14]. Although the present E_e dependence was too weak to insist that the periods showed broad maxima at E_e = 2–4 keV. However, the present results were not inconsistent with the previously reported results as shown by the dashed lines [14].

In contrast, the elongations decreased with temperature T as shown in Fig. 5 and depended on the electron energy E_e as shown in Fig. 6. That is, the elongations increased with increasing E_e and reached a maximum around E_e = 2 keV for low T and monotonically increased with increasing E_e (E_e < 5 keV) for high T.

We restrict here our discussion to the initial stage, before the start of the steady state of the layer-by-layer removal. The ESD scenario showed in the following [4,5,13]: The defects F and H centers are created from excitons by external electrons. The F* and H centers diffuse to the topmost surface. The H center emits interstitial halogen atom from the surface. The alkali atom is neutralized by an F center and is ejected. Simultaneously, the F center is replaced by the adjacent halogen atom. However this process is not possible for the flat surface for an energetic reason. Therefore, at the initial flat surface, F centers aggregate under the surface. Then the aggregated F (X) center formed under the surface initiates the formation of an initial pit. The F(X) centers work also to trap halogen atoms transported to the surface as H centers (i.e., F–H annihilation).

Although this scenario has been previously proposed, it is possible that the aggregation may elongate the initial half-period. Obvious elongations were observed in the present results. The right ordinates of Fig. 6 show the amount of the F centers accumulated in a few surface layers during the elongation (i.e., before the start of the steady state of the damping oscillation). The amount was calculated on the translation that the external electrons of the irradiation fluence for a period (1 ML removal) cause F centers to accumulate on the surface, whose number was equal to that of the alkali atoms on the topmost layer (5.0×10^{14} cm^{-2}). That is, if one extra period is present in the elongated region, the number of the F centers corresponds to 1 ML of alkali atoms. For 1.5 keV electrons, the elongation and estimated number of stored F centers were minimal in our work. In previous studies that verified the previously discussed scenario by 1 keV electron irradiation, the number of stored F centers in the surface layers had been estimated to a few percent of the number of alkali atoms on the surface [5,13].

The number of the F centers that accumulated in the surface layers are determined by the creation of F–H pairs and the diffusion of F* centers. With a simplified treatment, the relationship between the two could be taken into account by comparing the diffusion length of F* centers, λ_D, and the penetration depth of the external electron, l_P. The λ_D depends on the temperature T, whereas the l_P depends on the external electron energy E_e.

The T-dependent λ_D at 410 K was estimated to be 50 nm for the diffusion from the solid and 20 nm for the surface diffusion at E_e = 1 keV [9,13]. With elevating temperature, T, the diffusion of the F* centers was enhanced and λ_D increased (e.g., 100 nm for the surface diffusion at 470 K) [13]. Thus F* centers are easily encountered in the thin surface layers at high temperatures. Such encounters can enhance their accumulation. This is the reason why the elongations of the initial half-period decreased with elevating temperature T.

As for the E_e-dependent l_P, the deposit energy and number of holes as functions of penetration depth for 200–5000 eV external electrons were demonstrated previously [15]. As a rough estimate, the l_P's are 25, 50 and 100 nm for E_e = 1, 2 and 4 keV, respectively. This shows that the l_P's are comparable with λ_D and that external electrons with E_e = 1 keV create a large fraction of exicitons within λ_D, however, l_P increases over λ_D with increasing E_e. Thus, the fraction of F* centers that can reach the surface and aggregate, decreases as E_e increases. As the number of excitons created within λ_D does not increase so much, the

number of F* centers decreases with increasing E_e. It becomes more difficult for the F centers to aggregate, and the elongation lengthens as E_e increases.

Fig. 6 shows that this enhancement with E_e of the elongation reached its limit at $E_e = 2$ keV at low T. That is, the increase of the number of excitons created within λ_D reached its limit. At high T, the diffusion of the F* centers increases and λ_D also increases. Thus the F* centers created at deep positions could reach the surface and aggregate to the X centers. Therefore, at high T, the elongation decreases in the present range of E_e. Despite the overall small elongation for high T (Fig. 6(c)), the elongation continues to increase beyond $E_e = 5$ keV, where the external electrons become create F* centers at deeper positions. This fact is related to l_P. With increasing l_P in the present range of E_e, the F* centers become hard to reach surface and the elongation increases.

In contrast, the increase in the accumulated F centers at $E_e \leqq 2$ keV shown in Fig. 6 indicates that the effect of the surface diffusion is important for aggregation to the X centers. At $E_e = 1$ keV, the F* centers that diffused to the surface could also diffuse parallel to the surface after arriving at the surface and aggregate to an X center. A possible characteristic of the X centers is that they function as sinks of F* center-diffusion within the thin surface layer. Thus, the X centers become core for attracting F* centers that are quenched at the surface. Since the chance of an encounter between an X center and an F* center diffusing almost parallel to the surface in a thin region was large at the surface diffusion, the X centers grew effectively at $E_e = 1$ keV. The X centers in which the number of F centers that aggregated was less than several percent of the surface atoms could initiate the initial pits. By increasing E_e, the surface diffusion of F* centers and aggregation are suppressed. Therefore, despite the large number of F centers that accumulated and formed small X centers in the surface layer, surface erosion was not initiated at $E_e \geqq 2$ keV.

On the basis of the above interpretation, the temperature dependence shown in Fig. 5 can be understood as follows: At low T, as E_e increased to 2 keV, more than half the F* centers diffused to the surface and finished diffusing at the surface or in the solid. The immovable F centers were heaped under the surface and did not diffuse along it. A large number of immovable F centers blocked the thermal halogen diffusion because of F–H annihilation and a small fraction of F* centers aggregated to X centers at $E_e \geqq 2$ keV. At high T, because the F* centers could move easily, the number of immovable F centers stored in the bulk decreased. This resulted in a small elongation at high T.

Second, we discuss the steady state of the layer-by-layer removal, where the oscillation continued with a constant period. The ESD scenario showed the following [4,5,13]: In the steady state of the damping oscillation, the process of combining the F* centers and alkali atoms, and F–H annihilation become dominant. At that time, no further F centers aggregate. The movable F* centers arriving at the surface can neutralize and eject alkali atoms. This process depends on the number of atoms on the low-coordinate states. The number of F (F*) centers under the surface decreases with the increasing number of atoms on the low-coordinate states, and the pits grow their areas. Again the surface is flattened as the removal of one layer approaches, and the number of atoms on the low-coordinate states reduces to a minimum. The number of the F centers under the surface also increases as the one layer removal approaches. Under the flat surface, the concentrations of X and F centers are saturated to initiate the initial pits again.

Although the start of oscillation delayed in our results, after the start of steady-state oscillation, a large number of the F* centers combined with alkali atoms at low-coordinate states. The immovable F centers heaped under the surface worked to block the diffusion of H centers. Since the amount of the heaped F centers was around 30% of the number of atoms on the topmost layer, a considerable fraction of the H centers diffusing to the surface was blocked by them. The process continued the steady-state oscillation with a constant period.

The densities of the F centers in the topmost thin layer, N_1, and those heaped in the surface layers, N_2, can be written as functions of external electron fluence φ as follow;

$$dN_1/d\varphi = a_1\varphi - b_1(\varphi) - c_1(\varphi)N_1, \quad (1)$$

$$dN_2/d\varphi = a_2\varphi - b_2(\varphi) - c_2(\varphi)N_2, \quad (2)$$

where the first, second and third terms of the right-hand sides indicate the creation of F centers from the diffused F* centers, decrease of F centers via annihilation of F* centers by combination with alkali atoms, and annihilation of F centers by a recombination with H centers, respectively. The creation coefficients a_1 and a_2 are expected to be constant for φ. As for $b_1(\varphi)$, since the F* centers that combine with alkali atoms at low-coordinate states cannot become F centers, they decrease creation of F centers, $dN_1/d\varphi$, from the expected rate, $a_1\varphi$. In addition, if a pit erodes to the position of an F center in the topmost layer, the F center annihilates via the combination with an alkali atom of the pit-edge. Thus $b_1(\varphi)$ oscillates with φ, corresponding to the density of the low coordinated atoms and the density N_1 oscillates. Consequently, $c_1(\varphi)N_1$ oscillates depending on N_1 itself for the topmost layer. In contrast, for the F centers that heaped in the surface layers, $b_2(\varphi) = 0$, assuming that the variation of the amount of F* centers at the topmost surface layer does not give significant influence on N_2. In addition, $c_2(\varphi)$ is expected to be a constant for φ, because it depends only on the number of H centers simultaneously created with F* centers. Next, positive value of Eq. (2) increases N_2 and makes the right-hand side of Eq. (2) decreased, and *vice-versa*. Thus Eq. (2) may be approximated to 0 during the damping oscillation. Therefore the density N_2 is almost constant in the steady state.

The equations do not show the coupling process, where F centers heaped in the surface layers move to the topmost surface. Even if the density of F centers becomes large, we assume that the F centers are trapped in lattice sites and movable F* centers become to be F centers counted in N_1 or N_2. The F centers counted in N_1 can aggregate to X centers connecting with each other, when they are pasted by the F* centers diffused in the topmost surface layers. In addition, the X center grown at the surface would also take in the heaped F centers counted in N_2 lying near at the topmost layers. In this process, the F centers are pasted with the X center by F* centers arrived through the bulk diffusion. Via these X center growth processes, the repetition of the aggregation to the X centers occurs at the periodically flattened surface.

The equations show that the number of F centers shown in Fig. 6 indicates the number of F centers that accumulated in the topmost thin surface layers, N_1 and a part of N_2 (i.e., the number of heaped F centers taken in X centers) at $\varphi = \varphi_0$, which is the fluence at initiation. Thereafter, in each condition of T and E_e, $N_1(\varphi)$ oscillated with φ. Although the number of surface layers for containing N_2 depend on T and E_e, number of F centers, N_2, in many surface layers is quenched and remained almost constant for each condition of T and E_e, and correlats with the mean value of oscillating $N_1(\varphi)$ in the steady state.

Note that, in the previous work for $E_e = 1$ keV, the authors revealed the amounts of the stored F centers in a few periodic cycles as we stated in the previous section [5]. Their amounts of stored F centers oscillated with φ, which corresponded to the summation of our N_1 and N_2. The number of surface layers for containing N_2 for $E_e = 1$ keV was small compared with that of the present study.

Finally, we discuss monolayer pits creation by HCIs impact from viewing our results [6–8]. The number of desorbed atoms in the steady state is ~10 atoms/electron for $E_e = 2$ keV and $T = 440$ K, which is known from the periods shown in Figs. 4, or 2(b). The temperature, $T = 440$ K, is nearly equal to that treated in the work [6]. The results of the work showed that the number of the desorbed atoms was typically 2000 atoms, where the potential energy of the HCI was 15 keV [6]. If the pit was created only by electrons emitted from HCI via Auger decays, the number of bombarding electrons was simply estimated to be

200. Even if HCI emitted electrons via a multi-electron process, the number was somewhat large. In the previous work, an effect caused by much higher density of electrons than ordinary electron bombardment was discussed [6]. In this work, we stated that aggregated F center is created on the initial flat surface instead of the atomic emission and the shown number of the desorbed atoms/electron is only for the steady state. The number of electrons needed to initiate the formation of pits is $2 \times 10^{13}/cm^2$ as known from Figs. 6, or 2(b). From the fluence, it is estimated that 20 electrons/HCI bombarding the surface within an area of the pit size (10×10 nm^2) could create a pit. Since the energy of Auger electrons was small compared with $E_e = 2$ keV, the aggregation to X center might be more effective. This scenario shows that the Auger electrons could remove 100 atoms/electron by creating a pit on the flat surface. The high potential energy of HCI and high density of electrons should help F centers to aggregate to an X center.

5. Conclusion

The oscillations of specular yields of protons scattered on a KBr (0 0 1) ESD surface for 1.5–5 keV electron irradiation fluence were measured. In the oscillation, the first half-period elongated, and the elongation depended on the sample temperature and irradiation electron energy. From the extra electron fluence irradiated in the half-period, the number of F centers that accumulated in the thin surface layers during the elongation grew to 30% of the number of alkali atoms on the topmost layer. Our interpretation is that the X centers functioned as sinks of F* center-diffusion within the thin surface layer. It is expected that the X centers grew and bedded in numerous F centers under the flat surface before the initiation of surface erosion. Aggregation to the X center prior to steady-state oscillation occurred in the thin surface layers, where the density of the F and F* centers in the surface layers was quenched. With our results, we attempted to discuss the formation of the X center by HCI impact.

Declaration of Competing Interest

The authors declare that they have no known competing financial interests or personal relationships that could have appeared to influence the work reported in this paper.

Acknowledgments

We are grateful to Mr. Yuta Yoshikawa, one of our members, for his help of the experiments. This work was supported by JSPS KAKENHI Grant Number JP26790067 and Aid for young scientists from Osaka-Kyoiku University.

References

[1] Y. Kido, Surface Nano-structures Analysis by Photon, Electron and Ion Beams, Sankeisha, 2017, p. 541 (in Japanese).
[2] Y. Fukazawa, K. Kihara, K. Iwamoto, Y. Susuki, Nucl. Instr. Meth. B 315 (2013) 60.
[3] Y. Fukazawa, K. Kihara, K. Iwamoto, Y. Susuki, J. Vac. Soc. Jpn. 56 (2013) 428.
[4] M. Szymonski, J. Kolodziej, B. Such, P. Piatkowski, P. Struski, P. Czuba, F. Krok, Prog. Surf. Sci. 67 (2001) 123.
[5] B. Such, J. Kolodziej, P. Czuba, P. Piatkowski, P. Struski, F. Krok, M. Szymonski, Phys. Rev. Lett. 85 (2000) 2621.
[6] R. Heller, S. Facsko, R.A. Wilhelm, W. Möller, Phys. Rev. Lett. 101 (2008) 096102.
[7] R.A. Wilhelm, A.S. El-Said, F. Krok, R. Heller, E. Gruber, F. Aumayr, S. Facsko, Prog. Surf. Sci. 90 (2015) 377.
[8] R.A. Wilhelm, R. Heller, S. Facsko, EPL 115 (2016) 43001.
[9] M. Goryl, B. Such, F. Krok, K. Meisel, J.J. Kolodziej, M. Szymonski, Surf. Sci. 593 (2005) 147.
[10] Y. Fukazawa, R. Nakagawa, Y. Susuki, J. Vac. Soc. Jpn. 60 (2017) 153.
[11] Y. Fukazawa, R. Nakagawa, Y. Susuki, Vac. Surf. Sci. 61 (2018) 166.
[12] Y. Fukazawa, K. Tasaki, Y. Susuki, Vac. Surf. Sci. 62 (2019) 546 (in Japanese).
[13] J. Kolodziej, B. Such, P. Czuba, F. Krok, P. Piatkowski, P. Struski, M. Szymonski, R. Bennewitz, S. Schär, E. Meyer, Surf. Sci. 482–485 (2001) 903.
[14] Z. Postawa, J. Kolodziej, P. Czuba, P. Piatkowski, A. Poradzisz, M. Szymonski, J. Fine, Springer Series in Surface Sciences, Springer, Berlin, 1993, p. 299.
[15] M. Szymonsky, Det Kongelge Danske Videnskabernes Selskab, Mat.-fys. Medd. 43 (1993) 495.